Contribution from the Department of Chemistry,
The University of Chicago, Chicago, Illinois 60637

Can M_6X_8 Clusters Form Intercluster Metal-Metal Bonds?

Timothy Hughbanks*

Received August 20, 1985

M_6X_8 clusters are always found to form exo bonds to donor ligands. This behavior is simply understood in terms of the electronic structure of the cluster core: the LUMO orbitals of the clusters have a σ-acceptor character. These relatively low-lying orbitals should be available for intercluster metal-metal bond formation providing species can be made that have a formal cluster d-electron count greater than 24. Cluster dimers should be stable for 25 electrons per cluster, and 26 electrons per cluster is favorable for one-dimensional polymers. A cubic "Chevrel phase alternative" structure utilizing M_6O_8 clusters is promising in that the steric requirements of the oxo clusters allow the tight packing necessary for intercluster metal-metal bonding. A sampling of molecules and extended systems is treated, and analogies are drawn with known or potential B_6 species.

Introduction

The M_6X_8 cluster unit is a basic structural building block in an ever widening variety of inorganic compounds. The cluster has the highly symmetrical structure **1**, in which eight anions sit

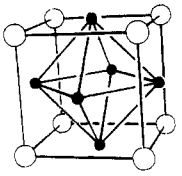

1

over the triangular faces of a metal octahedron. This type of cluster was first uncovered in the form of a $[Mo_6Cl_8]^{4+}$ species[1] and is the fundamental structural unit in α-$MoCl_2$. Terminal and two-coordinate bridging chlorides serve to cap the square faces of the cluster and stitch the solid-state structure together. The capping of the six square faces by ligands, hereafter referred to as "exo bonding", has subsequently proven to be a characteristic and constant feature of all M_6X_8 cluster compounds. In more recent years, the $[Mo_6X_8]^{4+}$ clusters (X = Cl, Br) have been shown to exhibit a fascinating photochemistry.[2] A chemistry of $[Nb_6I_8]^{n+}$ (n = 0, 2, 3) has been developed.[3] Ternary rhenium chalcogenides have been made[4] in which the $[Re_6X_8]^{4+}$ (X = S, Se) cluster is a basic structural component. The solid-state structures of these compounds are characterized by Re-X exo bonds involving sulfides, disulfides, or atoms of adjacent clusters. The closely scrutinized molybdenum chalcogenides also have rich chemistry involving $[Mo_6X_8]^{n-}$ (n = 0-4, X = S, Se, Te) clusters, which are found in compounds known as the "Chevrel phases".[5] In these materials, clusters are linked together by exo bonds to the chalcogens of neighboring clusters only—without any intervening sulfides or disulfides.[5d] The structure of the methoxide-supported cluster dianion $[Mo_6(\mu_3\text{-}OMe)_8(OMe)_6]^{2-}$ was recently determined to possess the same basic octahedral Mo_6 cluster inscribed in a cube of triply bridging methoxides with exobonded terminal methoxides.[6]

Two features that are common to all these systems are not difficult to identify. First, as noted above, M_6X_8 clusters are always exo-bonded to six capping donor ligands. Second, the formal cluster d-electron count does not exceed 24.[7] Earlier theoretical treatments make it clear how these two features are connected.[8] Twenty-four electrons is the optimal upper limit for metal-metal bonding in low-spin M_6X_8 clusters. Systems with more electrons will populate metal-metal antibonding orbitals, which lie above the bonding manifold over a significant gap; at least this is the case *when the cluster is exo-bonded to donors*. However, the cluster makes use of relatively low-lying dsp-hybrid orbitals in forming M-X exo bonds. In this paper we will explore the possibilities of using these orbitals for "making" metal-metal bonds between reduced clusters with electron counts greater than 24. Our conclusions are supported by calculations using the extended Hückel method. Mo parameters were used to represent a generic transition metal throughout, regardless of the electron count. As we shall see, rhenium parameters might have been more appropriate for certain systems. The differences to be expected are fairly small due to the adjacency of these elements' rows. For further details of the calculations see the Appendix.

Monomers, Dimers, and Chains

The electronic structure of M_6X_8 clusters has been a subject of numerous experimental and theoretical investigations.[8] Most of these studies have focused on the internal metal-metal bonding rather than on the capacities of the cluster to interact with exo-bonded ligands (or with metal atoms of other clusters). The molecular orbital diagram in Figure 1 emphasizes the frontier orbitals of a $Mo_6S_8^{4-}$ cluster, which, by virtue of their spatial extension, are utilized by the metals in the formation of exo bonds. The exo σ bonds of the octahedral cluster naturally span the a_{1g}, e_g, and t_{1u} representations, and the MO's illustrated in Figure 1 do indeed have these symmetries. As depicted, these orbitals are primarily built from the d_{z^2} atomic orbitals on each metal (each metal is presumed to lie at the origin of a local coordinate system such that the z axis is normal to the face of the cluster in which it resides). The a_{1g} MO is a low-lying metal-metal bonding orbital

* Present address: Department of Chemistry and Ames Laboratory, Iowa State University, Ames, IA 50011.

(1) The structure of $MoCl_2$ was reported in: (a) Schäfer, H.; von Schnering, H. G.; Tillack, J.; Kuhnen, F.; Wöhrle, H.; Baumann, H. *Z. Anorg. Allg. Chem.* **1967**, *353*, 281. The $Mo_6Cl_8^{4+}$ ion was first seen in $[Mo_6Cl_8](OH)_4 \cdot 8H_2O$. See: (b) Brosset, C. *Ark. Kemi, Mineral. Geol.* **1945**, *20*, No. 7.

(2) (a) Maverick, A. W.; Najcizionck, J. S.; Mackenzie, D.; Nocera, D. G.; Gray, H. B. *J. Am. Chem. Soc.* **1983**, *105*, 1878. (b) Nocera, D. G.; Gray, H. B. *J. Am. Chem. Soc.* **1984**, *106*, 824.

(3) (a) Simon, A.; von Schnering, H.-G.; Schäfer, H. *Z. Anorg. Allg. Chem.* **1967**, *355*, 295. (b) Imoto, H.; Simon, A. *Inorg. Chem.* **1982**, *21*, 308. (c) Stollmaler, F.; Simon, A. *Inorg. Chem.* **1985**, *24*, 168.

(4) (a) Spangenberg, M.; Bronger, W. *Angew. Chem.* **1978**, *90*, 382; *Angew Chem., Int. Ed. Engl.* **1978**, *17*, 368. (b) Chin, S.; Robinson, W. R. *J. Chem. Soc., Chem. Commun.* **1978**, 879. (c) Bronger, W.; Meissen, H.-J. *J. Less-Common Met.* **1982**, *83*, 29. (d) Leduc, P. L.; Perrin, A.; Sergent, M. *Acta Crystallogr., Sect. C: Cryst. Struct. Commun.* **1983**, *C39*, 1503. (e) Bronger, W.; Meissen, H.-J.; Müller, P.; Neugröschel, R. *J. Less-Common Met.* **1985**, *105*, 303.

(5) (a) Chevrel, R.; Sergent, M.; Prigent, J. *J. Solid State Chem.* **1971**, *3*, 515. A leading reference to the extensive literature of these compounds is: (b) Chevrel, R.; Gougeon, P.; Potel, M.; Sergent, M. *J. Solid State Chem.* **1985**, *57*, 25. See also reviews in: (c) *Topics in Current Physics: Superconductivity in Ternary Compounds I and II*; Fisher, O., Maple, M. B., Eds.; Springer-Verlag: New York, 1982. In $^1_\infty[Mo_6S_7]$, Mo_6S_8 clusters are *fused* along a 3-fold axis. See: (d) Gougeon, P.; Potel, M.; Padiou, J.; Sergent, M. *C. R. Seances Acad. Sci., Ser. 2* **1983**, *297*, 339.

(6) (a) Nanelli, P.; Block, B. P. *Inorg. Chem.* **1968**, *7*, 2423. The structures of these clusters were reported in: (b) Chisholm, M. H.; Heppert, J. A.; Huffman, J. C. *Polyhedron* **1984**, *3*, 475.

(7) Hamer, A. D.; Smith, T. J.; Walton, R. A. *Inorg. Chem.* **1976**, *15*, 1014. Compounds with the composition $Mo_6Cl_{11}(PR_3)_3$ were tentatively postulated to possess the 26-electron clusters $[(Mo_6Cl_8)(PR_3)_6]^{2+}$. Since these reduced clusters were formed with excess phosphine as the reducing agent, intercluster metal-metal bond formation would be inhibited by competition for open cluster faces.

(8) (a) Hughbanks, T.; Hoffmann, R. *J. Am. Chem. Soc.* **1983**, *105*, 1150. (b) Bursten, B.; Cotton, F. A.; Stanley, G. G. *Isr. J. Chem.* **1980**, *19*, 132 and references therein.

0020-1669/86/1325-1492$01.50/0

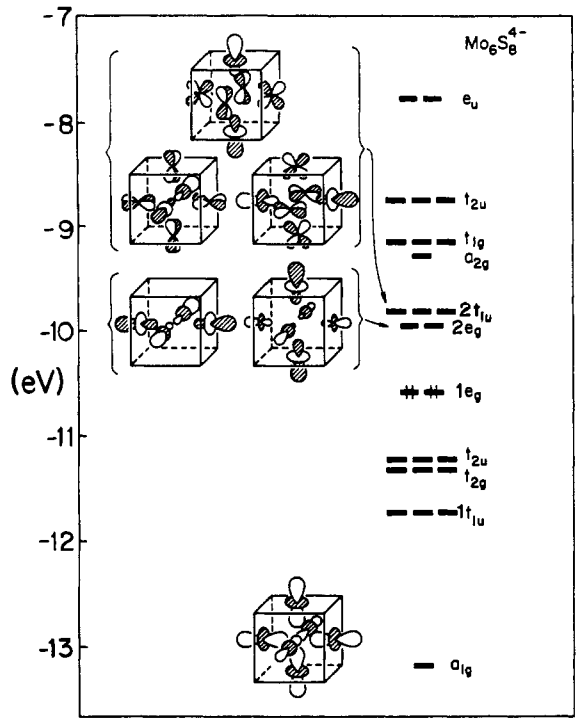

Figure 1. Molecular orbital diagram including the Mo-based orbitals for a $Mo_6S_8^{4-}$ cluster. Sulfur-based levels begin just below the a_{1g} orbital. The orbitals illustrated are those with a significant exo σ-bonding capacity. Electrons in the $1e_g$ orbital indicate the occupancy in a 24-electron cluster.

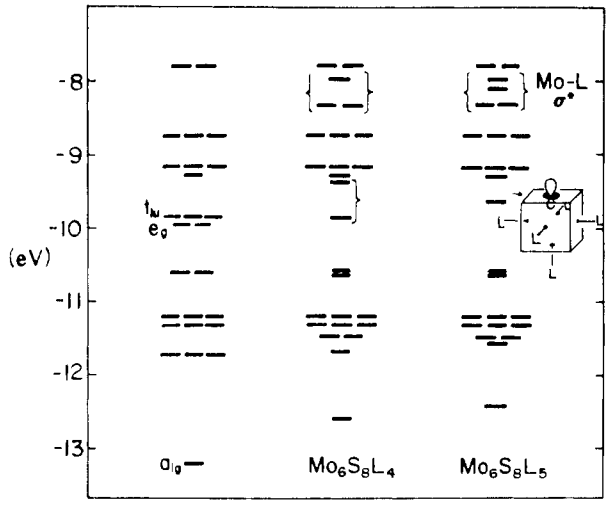

Figure 2. Diagram showing perturbation of the Mo_6S_8 MO's upon the ligation of simple σ donors. In $Mo_6S_8L_4$ the four ligands are in the equatorial basal plane; in $Mo_6S_8L_5$ the bottom apical site is ligated. Note that in $Mo_6S_8L_5$ a single exo-bonding frontier orbital remains relatively low in energy. Except for the a_{1g}, e_g, and t_{1u} orbitals, the metal–metal bonding orbitals are seen to be quite insensitive to ligation.

and includes Mo s and p hybridization so as to accentuate its bonding character. As discussed in previous work,[8] capping of the cluster with donor ligands pushes this orbital up somewhat, but this is largely compensated by increased Mo s and p hybridization that localizes the orbital amplitude more on the inside of the cluster (see **11** and the accompanying discussion below). Above the manifold of 12 metal–metal bonding orbitals, which are the occupied metal-based orbitals in "saturated" 24e clusters, sit the $2e_g$ and $2t_{1u}$ σ-acceptor orbitals (hereafter, the label of "2" will be dropped in referring to these orbitals). These orbitals also include some s and p hybridization, but in this case the hybridization acts to accentuate their projection outward from the cluster. When the cluster is capped by donor ligands, these orbitals are strongly destabilized as the occupied donor orbitals are stabilized; this is the essential driving force for the formation of dative exo M–X bonds.

Can the low-lying e_g and t_{1u} orbitals be utilized for *inter*cluster metal–metal bonding? In an attempt to answer to this question, calculations were performed on a dimer, $[Mo_6S_8L_5]_2$, and an infinite polymer, $^1_\infty[Mo_6S_8L_4]$. As represented in **2** and **3**, adjacent

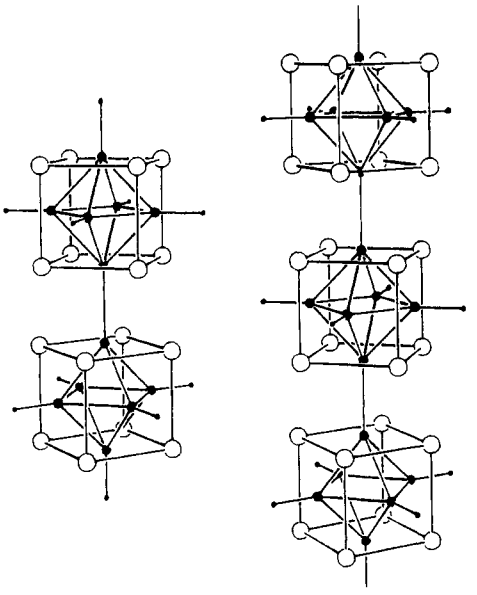

2 **3**

clusters are assumed to adopt a staggered orientation to minimize intercluster S--S repulsions. These systems are most easily analyzed in terms of the fundamental building blocks from which they are constructed, $Mo_6S_8L_4$ and $Mo_6S_8L_5$ fragments. For the purpose of computational economy, L was taken to be a model hydride ligand for which the H_{ii} value and orbital exponent were chosen to mimic an electronegative σ-donor (see the Appendix and ref 10). Figure 2 shows how the Mo_6S_8 cluster MO's are perturbed upon the successive addition of four basal ligands, followed by one apical ligand, to the vertices of the Mo_6 octahedron. Two components of the t_{1u} set and one component of the e_g acceptor orbitals strongly interact with the four basal ligands. The a_{1g} orbital is modestly destabilized by the ligand donors as well, though again this is partially compensated by s and p hybridization. These results are easily anticipated by inspection of the diagramatic MO illustrations of Figure 1; orbitals with d_{z^2} hybrids outwardly directed from the cluster faces are those pushed up by interaction with the added ligands. Note that, with the "top" and "bottom" faces of the clusters still exposed, there remain two low-lying acceptor orbitals, one each derived from the e_g and t_{1u} sets of the naked cluster and localized on the unsaturated Mo atoms.

The fifth ligand interacts with the two remaining acceptor orbitals of the $Mo_6S_8L_4$ species, with the net effect of pushing one orbital up and leaving a lone acceptor orbital behind. The orbital pushed up is a Mo–L antibonding combination and the remaining acceptor orbital is well localized on the last exposed Mo atom of the cluster (62%). This orbital is a nearly equal mixture of the two acceptor orbitals of the $Mo_6S_8L_4$ fragment as shown in **4**.

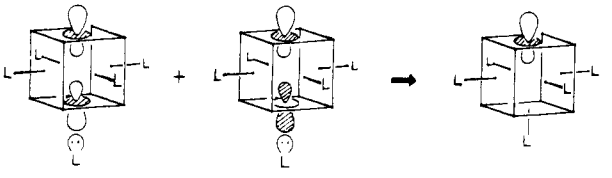

4

Intercluster bonding in the dimer **2** is the straightforward result of the interaction of two $Mo_6S_8L_5$ fragments as implied by Figure 3. The extent to which the interaction is limited to the mixing of the lone frontier hybrid orbitals is remarkable. Quite simply,

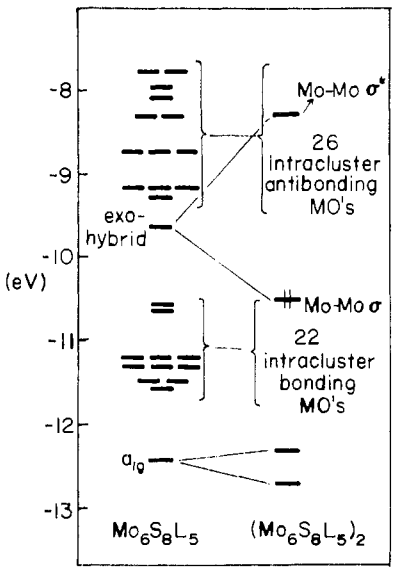

Figure 3. Orbital energy diagram of the interaction of two $Mo_6S_8L_5$ fragments. The interaction of the frontier exo hybrid orbitals leads to the formation of an intercluster Mo–Mo σ bond. The σ orbital is occupied (as shown) for a formal cluster electron count of 25.

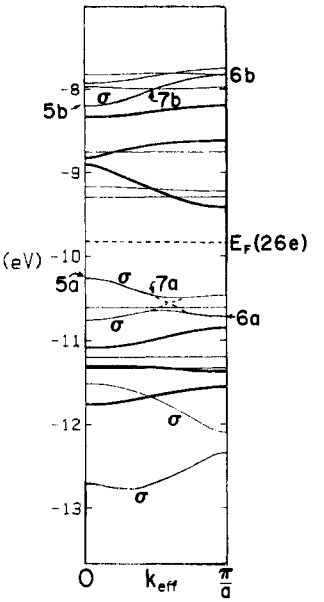

Figure 4. Electronic energy bands for a $Mo_6S_8L_4$ polymer. Heavy lines correspond to doubly degenerate bands. The meaning of "k_{eff}" is discussed in the text. Bands of the correct symmetry to incorporate intercluster Mo–Mo σ-bonding character are so marked. The labels **5a**, **5b**, etc. refer to crystal orbitals as discussed in the text and shown in illustrations with the corresponding labels.

these orbitals split to form bonding and antibonding levels so that the cluster HOMO–LUMO gap is essentially recovered. Not indicated in the figure is a small mixing between the deeply occupied a_{1g} derived orbitals and modest rehybridization between the a_{1g} orbitals and the frontier orbitals. The remainder of the cluster MO's are negligibly perturbed and the brackets indicate the extent of their energetic dispersion in the supermolecule. It is clear that the preferred formal cluster electron count is *25* (corresponding to a 1.17-eV gap in Figure 3). Perhaps the most likely synthesis of such a molecule should proceed via reductive coupling of a 24-electron $M_6X_8L_6$ species. The energy gained from the interaction of the two radical fragments is calculated to be 32 kcal/mol though this number is to be taken with caution due to the inherent limitations of the extended Hückel method and lack of any attempt to optimize the geometries of the "reactants" or "product".

The situation for the polymer **3** is slightly more complicated because there are *two* frontier orbitals for the $Mo_6S_8L_4$ fragment and because we must contend with band theoretic language rather the more familiar MO theory.[9] The electronic energy band dispersion curves for $^1_\infty[Mo_6S_8L_4]$ are shown in Figure 4. Although there are two clusters per unit cell, the eightfold screw axis threading the chain may be used to "unfold" the bands so that the band structure takes the appearance of corresponding to a one cluster per cell situation.[10] This has been done in Figure 4, and an "effective" wavevector (k_{eff}) determines the crystal orbital phase factors on moving from cluster to cluster upon the application of an eightfold screw operation. As examples, when $k_{eff} = 0$, the phase factor between crystal orbital coefficients of corresponding AO's on neighboring clusters is $e^{ik_{eff}a} = e^0 = 1$; when $k_{eff} = \pi/a$, the phase change is $e^{ik_{eff}a} = e^{i\pi} = -1$. As usual, dispersion curves for negative k_{eff} mirror positive values and are omitted from Figure 4. The region of "k_{eff}-space" between $-\pi/a$ and π/a will still be referred to as the "first Brillouin zone". Heavy lines in the figure correspond to doubly degenerate bands. There are 13 bands below a clear gap, indicating that the optimal Fermi level corresponds to a formal cluster electron count of 26.

Given the unbroken metal–metal-bonded network in the chain, one might have expected that the resulting system should inevitably be metallic, rather than semiconducting (with a computed band gap of 0.84 eV for the 26-electron case). There are two ways to understand this behavior, the first being a straightforward analysis of how the $Mo_6S_8L_4$ frontier fragment MO's will interact to form bands. The two fragment MO's have a σ pseudosymmetry with respect to the chain axis and so the intercluster bonding can be understood by restricting our attention to the bands with σ labels in Figure 4. Of the five bands so labeled, three descend from the uninteresting *intra*cluster bonding a_{1g}, $1t_{1u}$, and $1e_g$ molecular orbitals as required, given the lowering of the O_h symmetry of the free clusters to the axial 4-fold symmetry in the chain. Two remaining σ bands are predominantly derived from the $Mo_6S_8L_4$ fragment frontier orbitals. We can now deduce how the two exo-bonding frontier orbitals must mix for various values of k_{eff}. For $k_{eff} = 0$, the crystal orbitals must have the same phase from one cluster to the next. The mixing of the symmetric and antisymmetric frontier orbital combinations are as illustrated in **5a** and **5b**, respectively. For $k_{eff} = \pi/a$, the crystal orbitals are now constrained to be out of phase on adjacent clusters as illustrated in **6a** and **6b**. For $k_{eff} = \pi/2a$, crystal orbital phase factors must change sign every *two* clusters and consequently the symmetric and antisymmetric frontier orbital contributions are about equal in the bonding and antibonding band (**7a**,**b**). These crystal orbitals are indicated in Figure 4. Because the two frontier orbitals are nearly degenerate and the magnitude of all the intercluster overlaps between the frontier orbitals is comparable, the splittings within the pairs **5a**,**b**, **6a**,**b** and **7a**,**b** are nearly equal. Therefore the two bands resulting from the mixing of the $Mo_6S_8L_4$ cluster frontier orbitals are rather flat and remain below (above) the band gap due to their bonding (antibonding) character throughout the zone.

There is a second way to understand the flatness of the intercluster Mo–Mo σ bonding and antibonding bands and the resultant band gap. This is simply to recognize that orbitals *within* the sets {**5a**, **6a**, **7a**} and {**5b**, **6b**, **7b**} are nearly degenerate and we have two simple bands, σ and σ^*. Just as was true for the two $Mo_6S_8L_4$ fragment frontier orbitals, the rest of the cluster atoms do not split the *intra*cluster Mo_2 dimers' σ and σ^* molecular orbitals much.

A Cubic "Chevrel Phase Alternative"

Let us now consider a three-dimensional system in which M_6X_8 clusters may fully exploit their potential for intercluster metal–metal bond formation. The structure that most easily satisfies this requirement is illustrated in **8**. The clusters are merely packed

(9) For some treatments that are particularly accessible, see: (a) Gerstein, B. C. *J. Chem. Educ.* **1973**, *50*, 316. (b) Burdett, J. K. *Prog. Solid State Chem.* **1984**, *15*, 173. (c) Albright, T. A.; Burdett, J. K.; Whangbo, M.-H., *Orbital Interactions in Chemistry*; Wiley-Interscience: New York, 1985; Chapter 13.

(10) Hughbanks, T.; Hoffmann, R. *J. Am. Chem. Soc.* **1983**, *105*, 3528.

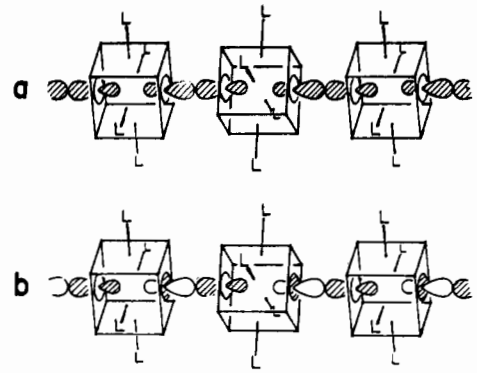

5

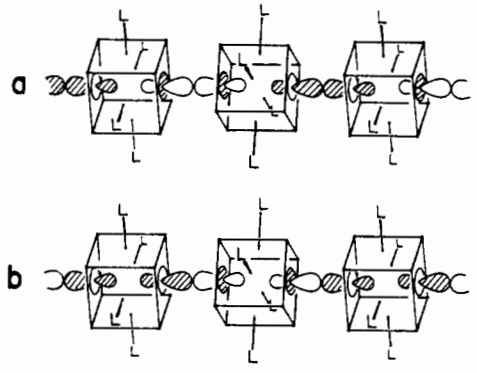

6

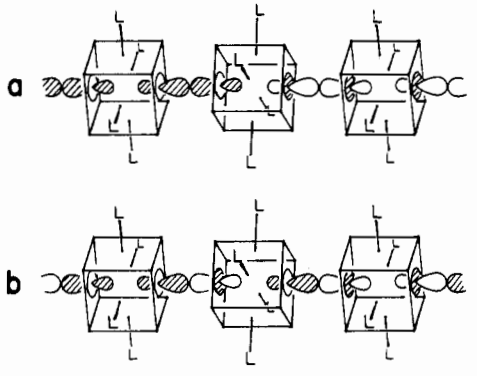

7

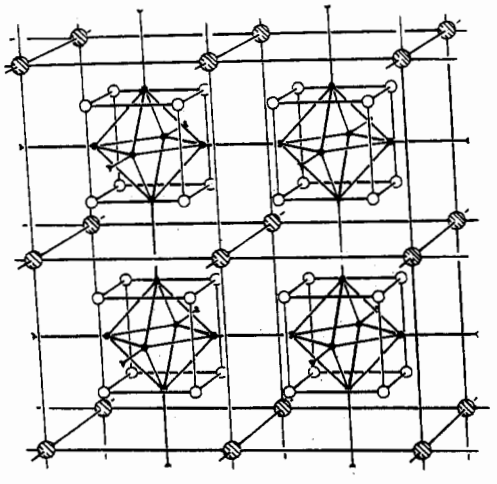

8

into a simple cubic array so that each cluster is face to face with its six neighbors; the remaining atoms in the structure may or may not be necessary and will be considered below. This structure is just a cubic alternative to the Chevrel phases, the latter can be

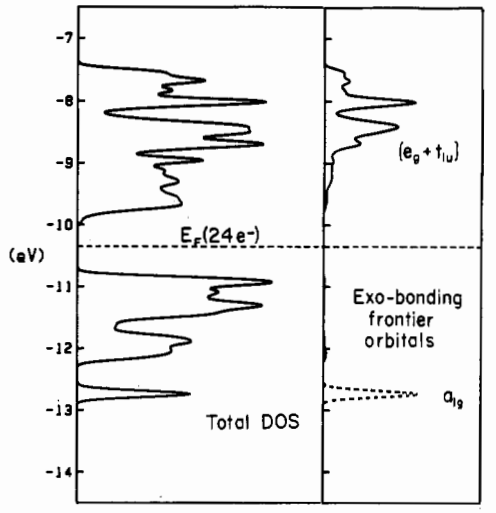

Figure 5. Density of states (DOS) curves for the rhombohedral Mo_6O_8 system (**8**). The energy range includes only the levels that are formally Mo bands; oxide s and p bands lie lower. As usual for a donor-capped M_6X_8 cluster system, the 24-electron occupancy corresponds to a semiconductor. The right panel illustrates how the contributions of the exo-bonding frontier orbitals are distributed. Note that the e_g and t_{1u} contributions are almost entirely in the unoccupied manifold.

generated by rotating each cluster by approximately 26° about the 3-fold axis of the cube in which it sits (see **9**) to yield the cluster

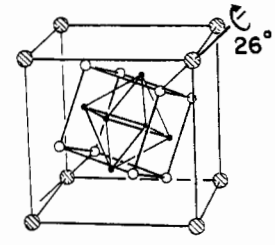

9

"packing" shown in **10**. These structures have been compared

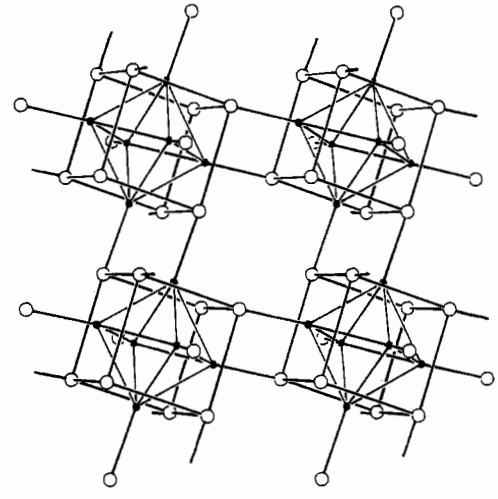

10

before. A study by Burdett and Lin[11] highlights an important steric constraint: for Mo_6X_8 (X = S, Se, Te) systems closed-shell repulsions between X atoms on neighboring clusters prevents the clusters from getting close enough to establish short intercluster Mo–Mo contacts. These steric constraints, often referred to as a "matrix effect" in discussing extended systems,[12] can be overcome. By use of the dimensions observed in $[Mo_6(\mu_3\text{-}OMe)_8$-

(11) Burdett, J. K.; Lin, J.-H. *Inorg. Chem.* **1982**, *21*, 5.
(12) Corbett, J. D. *Pure Appl. Chem.* **1984**, *56*, 1527; *J. Solid State Chem.* **1981**, *39*, 56.

$(OMe)_6]^{2-}$ for the Mo_6O_8 core, the structure in **8** can be assembled with intercluster Mo–Mo contacts equal to 2.54 Å *without* introducing any significant intercluster O–O repulsions (O–O = 3.08 Å). Furthermore, this cluster packing creates cubic cavities that will nicely accommodate an ion the size of Ba^{2+} or K^+ (at the positions of the shaded atoms in **8**). The question that remains is whether the metal–metal-bonded framework of **8** will be stable. If it is, for what electron count?

We will proceed by contrasting the rhombohedral and cubic alternatives. Calculations were performed on model systems in the rhombohedral (**10**) and cubic (**8**) geometries. In both cases the contents of the unit cell consisted of a Mo_6O_8 cluster in which the geometry observed for the core of the $[Mo_6(\mu_3\text{-}OMe)_8(OMe)_6]^{2-}$ ion was used.[13] In the rhombohedral geometry the lattice constant was 5.88 Å and the angle of rotation shown in **9** was 27.2°. This yields intercluster Mo–O and Mo–Mo contacts of 2.15 and 2.89 Å, respectively. In the cubic case the lattice constant was 6.13 Å and the intercluster Mo–Mo contacts were 2.54 Å. Further details of the band calculations are given in the Appendix.

The density of states for the rhombohedral Mo_6O_8 system displayed in Figure 5 is similar to that previously found for the Mo_6S_8 analogue.[8a] In the right panel of the figure, the contribution of the $e_g + t_{1u}$ and a_{1g} MO's is given and shows how these are destabilized by interaction with oxides on neighboring clusters. This *destabilization* of *unoccupied* levels is of course accompanied by the *stabilization* of *occupied* oxide-based levels, which is the essence of dative intercluster M–O bond formation. The $e_g + t_{1u}$ contribution in the *occupied* Mo d bands for a 24-electron system is negligible. The destabilization of the a_{1g} orbital is partially offset by an increase in Mo p hybridization that localizes the MO more on the "inside" of the cluster (see **11**). This leads to a very narrow

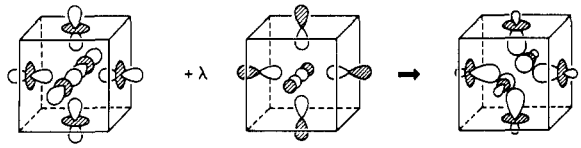

11

peak for the a_{1g} orbital because its interaction with neighboring clusters becomes quite small. This system shares the same general features as the previously studied Chevrel phases: excluding the a_{1g}, e_g, and t_{1u} exo hybrids, there is only moderate perturbation of the metal-localized d levels upon the "crystallization" of the clusters. The e_g and t_{1u} MO's continue to function as acceptors in the formation of intercluster M–O bonds.

The density of states changes markedly in the cubic case. First of all, the finite energy gap between metal–metal bonding and antibonding levels found for systems in which clusters are exo-bonded to donor ligands is no longer in evidence. However, Figure 6 shows that there is a pronounced local minimum in the density of states for a 28e/cluster.[14] For purposes of discussion we will assume the Fermi level to be at the 28-electron filling; further exploration of this choice will be found below. The right-hand panel of Figure 6 shows the projection of the a_{1g} and $e_g + t_{1u}$ exo hybrid MO's for this system to be quite different from the case where exo bonds involve non-metal donors. The a_{1g} peak is widened, and the $e_g + t_{1u}$ orbitals make a conspicuous contribution in the range below the Fermi level.

There is a simple way to capture the gist of these results if we utilize a less rigorous valence-bond interpretation. As we have seen, the a_{1g}, e_g, and t_{1u} orbitals depicted in Figure 6 are strongly perturbed in the formation of intercluster bonds. In the 24-electron

(13) The frontier orbitals of $Mo_6O_8^{4-}$ are similar to those of $Mo_6S_8^{4-}$. The e_g and t_{1u} orbitals lie somewhat higher in the bonding–antibonding gap for the oxo cluster. This may be related to the unusually long bonds Mo makes with the terminal methoxides in $[Mo_6(\mu_3\text{-}OMe)_8(OMe)_6]^{2-}$.[6b]

(14) A plot of the dispersion curves indicates that the 28-electron system is a "zero-gap" semiconductor (i.e., is semimetallic). However, in this instance the extended Hückel calculations are not accurate enough to be confident of this result.

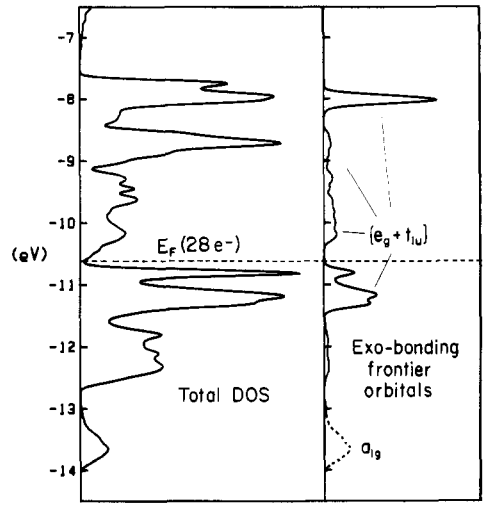

Figure 6. DOS curves for the cubic alternative Mo_6O_8 structure **10** in the same energy range as for Figure 5. While there is no band gap for this system, the 28-electron count corresponds to a deep local minimum in the total DOS. Note the contrast of the e_g and t_{1u} contributions with the rhombohedral case shown in Figure 5.

cluster there are two electrons among these orbitals—those in the low-lying a_{1g} orbital. We may imagine the construction of six *localized* hybrids from these six MO's. The procedure is entirely analogous to the construction of d^3sp^2 hybrids for a single octahedral center; the $\{d_{x^2-y^2}, d_{z^2}\}$ orbitals are of e_g symmetry, s is a_{1g}, and $\{p_x, p_y, p_z\}$ are t_{1u}. To form *homonuclear* bonds between clusters, we need to put one electron in each hybrid, or six electrons in all. Therefore, four electrons beyond the two already in the a_{1g} orbital for the 24e cluster are required. This scheme is summarized in **12**.

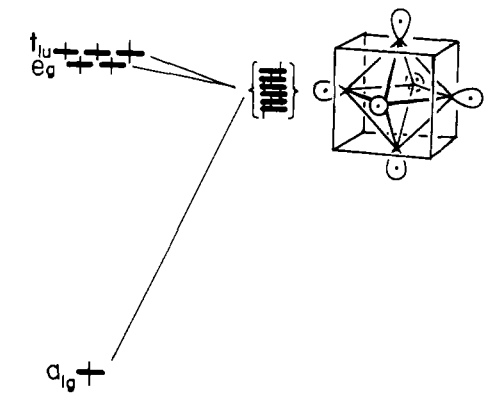

12

As with any simple outline, some important details have been missed. First, the role of the a_{1g} orbital is somewhat misrepresented. It does not "hybridize" with the e_g and t_{1u} orbitals to nearly the extent implied in the VB description. This may be surmised from inspection of the a_{1g} contribution shown in Figure 6; although this orbital gives rise to a wider band than was found for the rhombohedral case, it does not mix very much into other bands. In this respect, the situation is similar to that found for the dimer and chain systems discussed earlier. This misrepresentation is endemic to simple VB descriptions: the extent of hybridization among orbitals is too strongly dictated by geometrical constraints and the requirement of (2 center–2 electron) bond formation. Given the insignificant energy difference between e_g and t_{1u} fragment MO's it is not surprising that they mix strongly in forming intercluster bonding and antibonding orbitals. Because of the similarity between the e_g and t_{1u} contributions to the total DOS, they have simply been combined in Figure 6. A second fault with the simple VB description is the too neat consignment of "intercluster" and "intracluster" roles for metal–metal bonding given to the cluster MO's. We have not analyzed, for example,

Table I. Parameters for EH Calculations

	orb.	H_{ii}, eV	ζ_1 (c_1)[a]	ζ_2 (c_2)[a]
Hy	1s	−15.0	2.2	
B	2s	−15.2	1.30	
	2p	−8.5	1.30	
O	2s	−32.3	2.275	
	2p	−14.8	2.275	
S	3s	−20.0	2.12	
	3p	−13.3	1.83	
Mo	5s	−8.77	1.96	
	5p	−5.60	1.90	
	4d	−11.06	4.54 (0.5899)	1.90 (0.5899)

[a] Exponents: double-ζ d functions are used for molybdenum.

the effects of intercluster π interactions. The calculations indicate that this promotes slightly more mixing of "intracluster antibonding" MO's into the occupied manifold of bands of the crystal. This has the effect of sacrificing some *intra*cluster M–M bonding for *inter*cluster bonding.

Let us consider some of the more quantitative aspects of the calculations. The behavior of the calculated total energies for the cubic and rhombohedral structural alternatives reflects our previous discussion. For a 24e system, the rhombohedral structure is favored by (1.1 eV/cluster), whereas a 28e count favors the cubic alternative by (3.5 eV/cluster). Caution should be exercised in interpreting these numbers: the geometries are hypothetical and the calculations approximate. As we have discussed, an experimental realization of either structure is most likely to incorporate ions in the vacancies of these structures and will contribute importantly to their cohesive energies. Nevertheless, the trend favoring the cubic structure for the more electron-rich system is very strong. A compound such as $BaRe_6O_8$ could well adopt the cubic structure **8**. At the very least, the rhombohedral structure **10** would appear to be ruled out.

The overlap population data allow us to more closely examine the bonding in these structures (we will assume the Fermi level for the cubic and rhombohedral systems to correspond to 28 and 24 cluster electrons, respectively). Contrasting the intracluster bonding in the two structural alternatives, we find the Mo–Mo overlap populations to be 0.28 for the rhombohedral case and 0.22 for the cubic case. The values found for the $[Mo_6O_8]^{2-}$ and $[Mo_6(\mu_3\text{-}OH)_8(OH)_6]^{4-}$ species were 0.26 and 0.29, respectively. This indicates that although the capping of cluster faces with donor ligands may modestly enhance metal–metal bonding, the formation of intercluster metal–metal bonds comes partially at the expense of intracluster M–M bonds. In compensation, quite strong intercluster bonds are formed. The overlap population is calculated to be 0.54. Surprisingly, this *does not* necessarily mean that these bonds should be shorter than the intracluster bonds. Indeed, when a calculation was performed in which the cubic lattice constant was fixed and the intercluster Mo–Mo contacts were shortened from 2.54 to 2.4 Å while the intracluster contacts were lengthened to 2.63 Å, there was a destabilization of 0.5 eV/cluster. This is simply because there are *four* intracluster Mo–Mo bonds for every *one* intercluster bond. A similar trend is observed in the overlap populations for the $^3_\infty[B_6^{2-}]$ network in MB_6 compounds; overlap populations corresponding to bonds between B_6 clusters were twice as large as those within the clusters. Nevertheless, the bond lengths are comparable.

Conclusions

There are clear structural analogies between the systems investigated here and linked borane and carborane clusters, as well as with the extended MB_6 compounds. Indeed, taken alone, the metal framework in **8** is identical with the boron framework in CaB_6[15] and that of related lanthanide congeners. The treatment of exo bonding of borane clusters in terms analogous to those put forward in **12** is routine and quite reliable in the rationalization of borane structural chemistry. The coupling of boranes and carboranes via 2 center–2 electron bonds is not uncommon.[16] Decaborane(16) is a dimer of B_5H_8 fragments with an apex to apex B–B bond serving in the stead of the B–H bonds in the parent B_5H_9 molecule.[16a] Reduction of the closo anion $B_{10}H_{10}^{2-}$ yields the dimer $B_{20}H_{18}^{2-}$.[16b-d] Numerous carborane cage molecules have been linked as well.[16e] An analogous chemistry of M_6X_8 clusters should be feasible.

Acknowledgment. Thanks are due to the Dow Chemical Co. for their support of this research. I owe special thanks to Prof. J. K. Burdett for his support and encouragement.

Appendix

All the computations were carried out by using a program employing the extended Hückel method,[17a] which may be used for both molecular and crystal calculations. It has been developed to its present state by M.-H. Whangbo, S. Wijeyesekera, M. Kertesz, C. N. Wilker, C. Zheng, and the author. The weighted Wolfsberg–Helmholz formula[17b,c] was used for the H_{ij} matrix elements. Molybdenum parameters are from ref 18. Exponents for sulfur are from the tables of Clementi and Roetti,[19] and those of molybdenum originated with ref 20. In calculations on Mo_6S_8 cluster systems, all Mo–Mo distances were fixed at 2.705 Å and Mo–S distances were taken to be 2.40 Å. This is consistent with the choices made in ref 8a. The model hydrides (denoted by the symbol Hy in Table I) were bonded to Mo at a distance of 1.7 Å in all instances.

(15) For a leading reference on boron based nets see: Wells, A. F. *Structural Inorganic Chemistry*, 5th ed.; Oxford University Press: Oxford, England, 1984; Chapter 24.
(16) (a) Grimes, R.; Wang, F. E.; Lewin, R.; Lipscomb, W. N. *Proc. Natl. Acad. Sci. U.S.A.* **1961**, *47*, 996. (b) Hawthorne, M. F.; Pilling, R. L.; Stokely, P. F. *J. Am. Chem. Soc.* **1965**, *87*, 1893. (c) Schmitt, A. P.; Middaugh, R. L. *Inorg. Chem.* **1974**, *13*, 163. (d) Middaugh, R. L.; Wiersma, R. J. *Inorg. Chem.* **1971**, *10*, 423. (e) Plotkin, J. S.; Astheimer, R. J.; Sneddon, L. G. *J. Am. Chem. Soc.* **1979**, *101*, 4155 and references therein.
(17) (a) Hoffmann, R. *J. Chem. Phys.* **1963**, *39*, 1397. (b) Ammeter, J. H.; Bürgi, H.-B.; Thibeault, J. C.; Hoffmann, R. *J. Am. Chem. Soc.* **1978**, *100*, 3686. (c) Summerville, R. H.; Hoffmann, R. *J. Am. Chem. Soc.* **1976**, *98*, 7240.
(18) Kubáček, P.; Hoffmann, R.; Havlas, Z. *Organometallics* **1982**, *1*, 180.
(19) Clementi, E.; Roetti, C. *At. Data Nucl. Data Tables* **1974**, *14*, 177.
(20) Baranovskii, V. I.; Nikoiskii, A. B. *Teor. Eksp. Khim.* **1967**, *3*, 527.